Dyes and Pigments 88 (2011) 326–332

Contents lists available at ScienceDirect

Dyes and Pigments

journal homepage: www.elsevier.com/locate/dyepig

Novel derivatives of niclosamide synthesis: Its bioactivity and interaction with *Schistosoma japonicum* cercariae

Yong-Quan Wu [a,b], Tian-She Yang [b], Xun Li [a], Jun-Chen Wu [b], Tao Yi [b], Fu-You Li [b,*], Chun-Hui Huang [b], Xiao-Lin Fan [a,*]

[a] Key Laboratory of Organo-pharmaceutical Chemistry of Jiangxi Province, Gannan Normal University, Ganzhou, Jiangxi Province 341000, People's Republic of China
[b] Department of Chemistry, Fudan University, Shanghai 200433, People's Republic of China

ARTICLE INFO

Article history:
Received 18 February 2010
Received in revised form
2 August 2010
Accepted 2 August 2010
Available online 14 August 2010

Keywords:
Niclosamide derivative
4-Morpholin-1,8-naphthalimide
Schistosoma japonicum cercariae
Fluorescence imaging
Self-diffusion
Fluorescent labelling

ABSTRACT

Two novel niclosamide derivatives were synthesized by adding polyethylene glycol groups of differing lengths to a niclosamide core. The modified niclosamide derivatives were characterized using ^{1}H NMR and HRMS spectra. Anti-cercarial bioactivity results showed that the niclosamide derivative constructed to float on the surface of the water was able to kill cercariae when the number of hydrophilic groups was >3. A fluorescent niclosamide derivative containing naphthalimide was further synthesized to observe the interaction between the cercaricide and *Schistosoma japonicum* cercariae. Confocal fluorescence microscopy revealed that the fluorescent niclosamide derivative could easily penetrate into the cercarial body beyond the circulatory system leading to the rapid death of cercariae.

1. Introduction

Schistosomiasis is one of the burdensome and economic problems in endemic areas. The WHO estimates that 200 million people are infected and it is calculated that a further 600 million people are at risk of infection [1–5]. The cercarial stage of the Schistosome lifecycle is the only infectious stage. The cercarial stage is also the most fragile stage in the life cycle of *schistosome* [6]. More than 98% of cercariae float on the water surface, so it is possible to effectively control the risk of cercariae infection by the use of a thin cercaricide film floated on the water.

Niclosamide (see Scheme 1, compound **1**) has a long track-record as a killer of the tapeworm and snails that harbor *Schistosome* [7]. Moreover, niclosamide can effectively prevent *Schistosoma japonicum* cercariae from entering a human host by rendering cercariae uninfective with very short contact time [8]. Unfortunately, niclosamide has low water solubility, so a lot of work focuses on improving the solubilization of niclosamide [9,10]. However, no work on the improvement of the film floating properties has been reported.

Fluorescence imaging has been used as a powerful tool in the study of medicine and bioscience, including parasitology [11–13], especially in investigating the interaction between drugs and parasites *in vitro* and *in vivo*. Recently, fluorescence imaging in anti-parasite drug assaying has attracted much interest, and some possible modes of drug action have already been researched, such as an antiplasmodial drug [14]. However, niclosamide's mechanism of action was unknown in *S. japonicum* cercariae [15], our intention was to use fluorescence imaging technology to elucidate the preliminary interaction between niclosamide derivatives and *S. japonicum* cercariae. Our exploration focused on synthesizing novel cercaricides of niclosamide that can self-diffuse on the water surface and rapidly kill *S. japonicum* cercariae.

Herein, novel derivatives of niclosamide (see Scheme 1, **2a** and **2b**) were synthesized by coupling with polyethylene glycol (PEG). Compounds **2a** and **2b** have good bioactivity against *S. japonicum* cercariae, while **2b** possesses properties of self-diffusion and surface film formation at the air water interface. Furthermore, to obtain a rudimentary understanding of the mode of interaction of **2a** and the *S. japonicum* cercariae *in vivo*, a novel fluorescent compound **3** was synthesized by coupling a fluorophore

* Corresponding authors. Tel.: +86 797 8393536, +86 21 55664185; fax: +86 797 8393536, +86 21 55664621.
E-mail addresses: fyli@fudan.edu.cn (F.-Y. Li), vanxl@gnnu.edu.cn (X.-L. Fan).

0143-7208/$ – see front matter © 2010 Elsevier Ltd. All rights reserved.
doi:10.1016/j.dyepig.2010.08.002

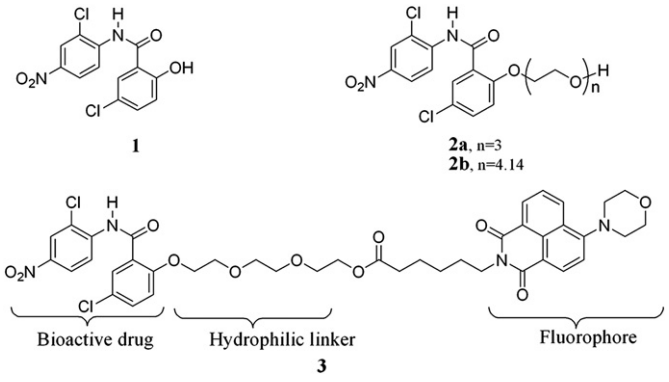

Scheme 1. Structures of niclosamide **1**, novel niclosamide derivatives **2** (**2a** and **2b**) and fluorescent compound **3**, $n = 4.14$ is the average degree of polymerization of PEG.

N-hexanoic acid-4-morpholin-1, 8-naphthalimide (compound **6**, Supplement Materials, Scheme S1) to niclosamide derivative **2a**. The interaction of **3** with *S. japonicum* cercariae was further investigated by confocal fluorescence microscopy.

2. Experimental section

2.1. Materials and instrumentations

All starting materials (reagents and solvents) were obtained from commercial supplies and used as received. Niclosamide was purchased from Huainan 3rd Pharmaceutical Factory (China). The KB cell lines were provided by Institute of Biochemistry and Cell Biology (China). Infected *Oncomelania hupensis* snails were supplied by Hunan Institute of Parasitic Diseases (WHO collaborating center for *Schistosomiasis* control in lakes).

^{1}H NMR and ^{13}C NMR spectra were recorded on a Mercuryplus spectrometer at 400 MHz and 100 MHz, respectively. Electrospray ionization mass spectra (ESI-MS) were measured on a Bruker APEX II FT-ICRMS 4.7T system. UV–visible spectra were recorded on a Shimadzu UV-2550 spectrometer. Fluorescence spectra were measured on an Edinburgh LFS920 fluorescence spectrophotometer. Fourier transform infrared (FT-IR) spectra were measured using a Nicolet Nexus 470 spectrometer with KBr pellet or film. Melting points were determined on a hot-plate melting point apparatus XT4-100A without correction. Fluorescence imaging experiments were performed on an OLYMPUS FV1000 IX81 confocal fluorescence microscope equipped with a 40× oil-immersion objective lens, excitation at 405 nm was carried out with a semiconductor laser and emission was collected at 480 to 580 nm. Observations of anti-*Schistosoma* cercariae experiments were performed on a XSZ-CTV biological microscope with Color TV Screen. BAM imaging experiments were performed with a JB04-Brewster angle microscope, equipped with a 30 mW laser emitting light at a wavelength of 532 nm, was used to visualise the structure of drug layers.

2.2. Synthesis

2.2.1. Toluene-4-sulfonic acid-2-[2-(2-hydroxy ethoxy) ethoxy]ethyl ester (**4**)

4 was synthesized as described previously [16]. IR (KBr) cm^{-1}: 3404, 3062, 2920, 2870, 1598, 1454, 1355, 1177, 1122, 1100, 817, 664. ^{1}H NMR (400 MHz, $CDCl_3$): δ 7.80 (d, 2H, $J = 8.4$ Hz, Ar–H), 7.34 (d, 2H, $J = 8.0$ Hz, Ar–H), 4.17 (t, 2H, $J = 4.8$ Hz, $-OCH_2$), 3.69–3.73 (m, 4H, $-OCH_2CH_2O-$), 3.57–3.61 (m, 6H, $-CH_2O-$), 2.45 (s, 3H, $-CH_3$), 2.22 (s, 1H, -OH). HR-MS: Calcd. for $C_{13}H_{21}O_6S$: 305.1059, $[M + H]^+$. Found: 305.1055.

2.2.2. 2-[2-(2-hydroxyethoxy)ethoxy]ethoxyl niclosamide (**2a**)

2a was synthesized according to the literature procedure [17,18]. Niclosamide (2.0 g, 6 mmol) was dissolved in 1, 4-dioxane (10 mL) at 85 °C in a 50 mL three-neck flask. K_2CO_3 (0.85 g, 6 mmol) and Bu_4NBr (0.20 g, 6 mmol) were added with stirring. **4** (1.55 g, 5 mmo1) dissolved in l, 4-dioxane (8 mL) was added dropwise and the ensuing mixture was heated under reflux for 6 h, and allowed to cool. Water (20 mL) was then added and the mixture was shaken in a separating funnel. The organic phase was separated, and the water phase extracted with CH_2Cl_2 (20 mL × 3). The combined organic layer was dried over anhydrous Na_2SO_4. After removing the solvent under reduced pressure, the crude product was purified by column chromatography, and a slightly yellow solid **2a** was obtained. Yield 78%. mp 84–86 °C. IR (KBr) cm^{-1}: 3458, 3385, 3272, 3104, 2952, 2905, 2854, 1674, 1589, 1561, 1503, 1471, 1207, 1113, 818, 744, 648. ^{1}H NMR (400 MHz, $CDCl_3$): δ 10.58 (s, 1H, –NH–CO–), 8.83 (d, 1H, $J = 7.2$ Hz, niclosamide-H), 8.31–8.32 (d, 1H, $J = 2.4$ Hz, niclosamide-H), 8.21–8.22 (d, 1H, $J = 2.4$ Hz, niclosamide-H), 8.17–8.20 (dd, 2H, $J = 2.4$ Hz, niclosamide-H), 7.45–7.48 (dd, 1H, $J = 2.4$ Hz, niclosamide-H), 7.07–7.09 (d, 1H, $J = 8.8$ Hz, niclosamide-H), 4.45–4.47 (t, 2H, $J = 4.8$ Hz, $-CH_2O-$), 3.92–3.95 (t, 2H, $J = 4.8$ Hz, $-CH_2O-$), 3.63–3.65 (t, 4H, $J = 4.8$ Hz, $-OCH_2CH_2O-$), 3.56–3.58 (t, 2H, $J = 4.8$ Hz, $-OCH_2-$), 3.49–3.51 (t, 2H, $J = 4.8$ Hz, $-OCH_2-$), 2.11 (s, 1H, –OH). HR-MS: Calcd. for $C_{19}H_{21}Cl_2N_2O_7$: 459.0726, $[M + H]^+$. Found: 459.0712.

2.2.3. Polyethylene glycol 200-ethoxyl niclosamide (**2b**)

The snthesis and separation methods for **2b** were similar to those adopted for **2a**, and a slight yellow liquid was obtained. Yield 60%; ^{1}H NMR (400 MHz, $CDCl_3$): δ 10.58 (s, 1H, –NH–CO–), 8.84–8.86 (d, 1H, $J = 7.2$ Hz, niclosamide-H), 8.32–8.34 (d, 1H, $J = 2.4$ Hz, niclosamide-H), 8.21–8.23 (d, 1H, $J = 2.4$ Hz, niclosamide-H), 8.19 (d, 2H, $J = 2.4$ Hz, niclosamide-H), 7.46–7.49 (dd, 1H, $J = 2.4$ Hz, niclosamide-H), 7.10–7.12 (d, 1H, $J = 8.8$ Hz, niclosamide-H), 4.46–4.48 (t, 2H, $J = 4.8$ Hz, $-OCH_2-$), 3.92–3.93 (t, 2H, $J = 4.8$ Hz, $-CH_2O-$), 3.49–3.65 (m, $-OCH_2CH_2O-$). HR-MS: Calcd. for $C_{23}H_{29}Cl_2N_2O_9$: 547.1250, $[M + H]^+$, $n = 5$, **2b** was further purified by column chromatography. Found: 547.1243.

2.2.4. [Toluene-4-sulfonic acid-2-(2-ethoxy)ethoxy ethyl ester] niclosamide (**5**)

An anhydrous CH_2Cl_2 solution (10 mL) of compound **4** (0.46 g, 1 mmol) and Et_3N (2 mL), was stirred at 0–5 °C to which was added tosyl chloride (0.38 g, 2 mmol) dropwise. The ensuing mixture was stirred for 10 h at room temperature, the solvent was removed under reduced pressure and the residue was subjected to column chromatography on silica gel. The product was separated with pure CH_2Cl_2, yielding a slightly yellow solid. mp 99 °C. Yield 51%. IR (KBr) cm^{-1}: 3288, 3079, 2908, 2874, 1676, 1546, 1509, 1475, 1342, 1174, 1119, 1096, 819, 744, 659. ^{1}H NMR (400 MHz, $CDCl_3$): δ 10.61 (s, 1H, –NH–CO–), 8.83–8.85 (d, 1H, $J = 9.2$ Hz, niclosamide-H), 8.32–3.33 (d, 1H, $J = 2.4$ Hz, niclosamide-H), 8.23–8.24 (d, 1H, $J = 2.8$ Hz, niclosamide-H), 8.20–8.21 (m, 1H, $J = 2.8$ Hz, niclosamide-H), 7.76–7.77 (d, 2H, $J = 8.4$ Hz, tosyl-H), 7.47–7.50 (m, 1H, $J = 2.8$ Hz, niclosamide-H), 7.33 (d, 2H, $J = 8.4$ Hz, tosyl-H), 7.10 (d, 1H, $J = 8.8$ Hz, niclosamide-H), 4.45–4.47 (t, 2H, $J = 4.8$ Hz, $-CH_2O-$), 4.07–4.09 (t, 2H, $J = 4.8$ Hz, $-CH_2O-$), 3.93–3.95 (t, 2H, $J = 4.8$ Hz, $-CH_2O-$), 3.59–3.61 (t, 4H, $J = 4.8$ Hz, $-OCH_2-$), 3.52–3.54(t, 2H, $J = 4.8$ Hz, $-OCH_2-$), 2.44 (s, 3H, tosyl-CH_3). HR-MS: Calcd. for $C_{26}H_{27}Cl_2N_2O_9S$: 613.0814, $[M + H]^+$. Found: 613.0804.

*2.2.5. [6-(N-hexanoic acid-4-morpholin-1,8-naphthalimide)-2-(2-ethoxy) ethoxy ethyl ester] niclosamide (**3**)*

N-hexanoic acid-4-morpholin-1, 8-naphthalimide (**6**) was synthesized according to the literature [19]. **6** (0.066 g, 0.17 mmol), **5** (0.127 g, 0.2 mmol) and K_2CO_3 (0.046 g, 0.33 mol) were mixed in acetone (15 mL) and stirred for 24 h under a nitrogen atmosphere at 50 °C. The solvent was removed under reduced pressure and the residue was subjected to column chromatography (dichloromethane/ethyl acetate = 5/2, v/v) on silica gel to yield compound **3** as a yellow solid. Yield 57%. mp 56–58 °C. IR (KBr) cm^{-1}: 3329, 2950, 2893, 2854, 1733, 1691, 1652, 1588, 1543, 1505, 1212, 1122, 1106, 1042, 901, 784. ^1H NMR (400 MHz, $CDCl_3$): δ 10.60 (s, 1H, –NH–CO–), 8.82–8.84 (d, 1H, J = 9.2 Hz, niclosamide-H), 8.55–8.57 (d, 1H, J = 6.0 Hz, naphthalimide-H), 8.49–8.51 (d, 1H, J = 8.0 Hz, naphthalimide-H), 8.40–8.42 (d, 1H, J = 8.4 Hz, naphthalimide-H), 8.31–8.32 (s, 1H, J = 2.4 Hz, niclosamide-H), 8.21–8.22 (d, 1H, J = 2.8 Hz, niclosamide-H), 8.17–8.20 (dd, 1H, J = 7.6 Hz, naphthalimide-H), 7.68–7.71 (d, 1H, J = 7.6 Hz, naphthalimide-H), 7.45–7.48 (d, 1H, J = 8.8 Hz, niclosamide-H), 7.21–7.23 (d, 1H, J = 8.0 Hz, niclosamide-H), 7.09–7.11 (d, 1H, J = 8.8 Hz, niclosamide-H), 4.46–4.48 (t, 2H, J = 4.8 Hz, $-CH_2O-$), 4.12–4.18 (m, 4H, $-CH_2O-$), 4.02 (t, 4H, J = 4.8 Hz, morpholin-H), 3.94–3.96 (t, 2H, J = 4.8 Hz, $-CH_2O-$), 3.64–3.66 (t, 2H, J = 4.8 Hz, $-CH_2O-$), 3.60–3.62 (t, 2H, J = 4.8 Hz, $-CH_2O-$), 3.56–3.58 (d, 2H, J = 5.6 Hz, $-CH_2-$), 3.25–3.28 (t, 4H, J = 4.8 Hz, morpholin-H), 2.32–2.35 (t, 2H, J = 7.6 Hz, $-CH_2-$), 1.66–1.70 (m, 4H, $-CH_2CH_2-$), 1.41–1.49 (m, 2H, $-CH_2-$). ^{13}C NMR (100 MHz, $CDCl_3$): δ 173.4, 164.3, 163.9, 162.5, 155.6, 155.4, 143.0, 141.2, 133.8, 132.5, 132.4, 131.1, 130.0, 129.8, 127.5, 126.1, 125.8, 124.7, 123.4, 123.3, 123.1, 122.6, 121.5, 117.1, 115.2, 114.9, 70.8, 70.5, 69.9, 69.2, 69.1, 67.0, 66.2, 53.4, 40.0, 34.1, 27.7, 26.6, 24.6; HR-MS: Calcd. for $C_{41}H_{43}Cl_2N_4O_{11}$: 837.2305, $[M+H]^+$. Found: 837.2306.

2.3. Photophysical properties and n-octanol/water partition coefficients

The UV–vis and fluorescence emission spectra of compound **3** in CH_2Cl_2 were studied, and fluorescence quantum yields of compound **3** were determined using quinine sulfate as a standard (yield = 0.53, in 0.1 M H_2SO_4, λ_{ex}: 365 nm).

n-Octanol/water partition coefficients of **1**, **2a** and **2b** were determined by the 'shake flask' direct measurement method. The saturated solutions were placed in an ultrasound bath for 30 min, then left to settle for 5 h. The absorbances of different solutions with the different compounds were determined. The partition coefficients were obtained by calculating the ratio of the absorbances of organic layers to water layers. Results are listed as log $K_{o/w}$ in Table S1.

2.4. Anti-cercarial activity experiments

Compound **3** was dissolved in dimethyl sulphoxide (DMSO), and diluted into concentrations with distilled water as follows: 2.6 μM, 3.60 μM, 7.00 μM, 9.80 μM and 13.7 μM. *S. japonicum* cercariae were collected from the infected *O. hupensis*. The snails were induced to shed cercariae by exposing them to bright light for 2 h, and cercariae were then transferred by metal spatula from the water surface to a plate containing a dilute solution of compound **3**, the activity of the cercariae was explored by biological microscopy at 8 h, 12 h, 15 h and 18 h. The exploring method for compound **2b** was analogous to that for compound **3**. The results are shown in Table S2 and Table 1.

2.5. Cell and cercaria imaging experiments

KB cells were plated on 18 mm glass coverslips in an atmosphere of 5% CO_2, 95% air at 37 °C to adhere for 24 h. Then the KB cells were stained with a 2.5 μM compound **3** solution in DMSO/PBS (v/v, 1:399) buffer for 15 min.

Cercariae were suspended in 200 μL solution of compound **3** on a special plate for imaging. At last, fluorescence imaging of cercariae was explored by confocal microscopy at 10 min, 30 min, 1 h, 2 h and 4 h. The control fluorophore **6** was dissolved in DMSO, and portioned into dilute solutions of 5 μM; the fluorescence imaging method was analogous to that for compound **3**.

Table 1
The mortality rate of *Schistosoma japonicum* cercariae for the cercaricide **2b** (25 °C).

Concentration (mg m^{-2})	Number of cercariae	Mortality (%)			
		30 min	60 min	90 min	120 min
1330.0	18	100	100	100	100
660.0	17	88	100	100	100
330.0	15	75	100	100	100
170.0	21	4	90	95	100
40.0	80	0	81	87	90
Blank	31	0	0	0	0

3. Results and discussion

3.1. n-Octanol partition coefficients

The partition coefficients were investigated by measurement of absorbances of **1**, **2a** and **2b** between water layer and n-octanol layer, and the data are shown in Table S1 (Supplement Materials). Compound **1** (niclosamide) was more lipophilic with logarithm of partition coefficient, log ($K_{o/w}$), of 3.53. The lipophilicity of **2a** and **2b** differed from **1** (log ($K_{o/w}$), 3.10 for **2a**, 2.96 for **2b**), because **2a** and **2b** have the hydrophilic polyethylene glycol (PEG) linker. These results indicated that our modification method improves the water solubility of niclosamide. However, because the water-surface floating property of **2b** (Supplement Materials, Fig. S1) is better than that of **2a**, the evaluation of the anti-Schistosoma cercariae experiment focused on **2b**.

3.2. Anti-cercarial activity experiments

The evaluation of cercaricide **2b** against cercariae was based on properties of self-diffusion and water-surface floating suitable to application in the field. The mortality rate of *S. japonicum* cercariae for **2b** was high, not only at a high concentration of 1330 mg m^{-2} but also at a low concentration of 40 mg m^{-2} (Table 1). For example, at a low concentration of 40 mg m^{-2} the mortality reached 95% at 120 min, which implies that the cercaricide **2b** maintained excellent bioactivity against cercariae in spite of the hydroxyl group of niclosamide being replaced by the PEG linker.

3.3. The fluorescent niclosamide derivative 3

3.3.1. UV–vis and fluorescence emission spectra

To monitor the activity of **2a** in living cercariae, **2a** was conjugated by fluorescent *N*-hexanoic acid-4-morpholin-1, 8-naphthalimide [20–22], and a novel niclosamide derivative **3** was synthesized. Furthermore, the chemical structure was confirmed by IR, ^1H NMR, ^{13}C NMR and HRMS spectra (Supplement Materials, Figs. S6–S9). The photophysical properties of **3** were investigated. The UV–vis absorption and fluorescence emission spectra of **3** in a dilute solution of CH_2Cl_2 were studied and are shown in Fig. 1. Derivative **3** exhibits a broad UV–vis band and maximal absorbance at wavelengths of 332 nm and 400 nm, corresponding to the π–π^* transition of niclosamide and fluorophore **6**, respectively. Under

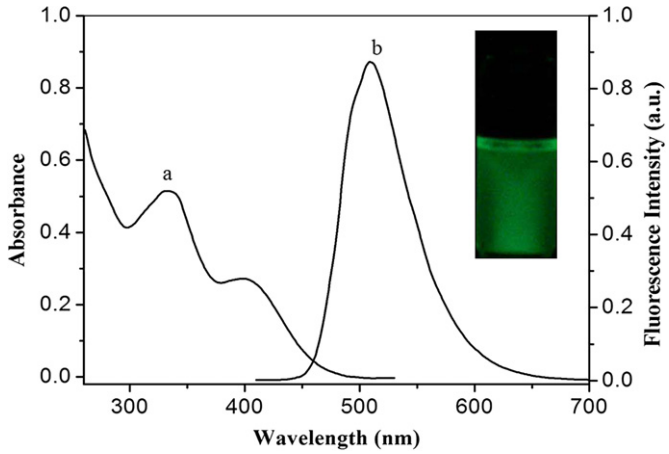

Fig. 1. UV–vis absorption (a) and fluorescent emission spectra (b) of compound **3** (10 μM) in CH_2Cl_2.

excitation at 400 nm, **3** emits green fluorescence at a maximum wavelength of 509 nm. The fluorescence quantum yield of **3** in CH_2Cl_2 solvent was measured to be 0.11 using quinine sulfate as a standard.

3.3.2. Anti-cercarial activity experiments

The bioactivity of **3** against cercariae was also tested before using this compound as a valid alternative for the investigation of the mechanism by which cercariae are killed. Mortality of *S. japonicum* cercariae was investigated by incubating with **3** *in vitro* and the results are shown in Table S2 (Supplement Materials). The experiment results show that **3** was also effective in killing the cercariae, because the mortality of *S. japonicum* cercariae reached the 95% at 7.00 μM concentration of **3**. In the control (blank of compound **3**), no cercariae were killed. Thus, **3** with its bioactivity, against cercariae, could serve as a potential fluorescent derivative for investigating niclosamide's mechanism of action in *S. japonicum* cercariae, although the anti-cercarial activity of **3** (7.00 μM, 3.5 mg L^{-1}) is lower than that of parent niclosamide under same condition (100% of cercariae were killed when they were immersed in niclosamide (0.3 μM, 0.1 mg L^{-1})) [23].

3.4. Cell imaging

In view of its favorable spectroscopic properties, **3** should be suitable for fluorescence imaging in living cells. As determined by confocal fluorescence microscopy, KB cells stained with a 2.5 μM solution of **3** in DMSO/PBS buffer (v/v, 1:399) for 15 min showed significant intracellular fluorescence (Fig. 2). The overlay of fluorescence and bright-field images revealed that the fluorescence signal localized in the intracellular region. Moreover, quantization of the fluorescence intensity profile of cells stained with **3** revealed that an extremely high signal ratio was associated with the cytoplasm of live cells (Fig. 2d), as indicated by the fluorescence signal ratio in the cytoplasm being above 3000 counts (region 1 and region 3) and that in the nucleus being about 5 counts (region 2). These results indicated that **3** was cell-permeable.

3.5. Cercaria imaging

Fresh cercariae labelled with **3** (5 μM) were observed using confocal fluorescence microscopy. The fluorescence labelling

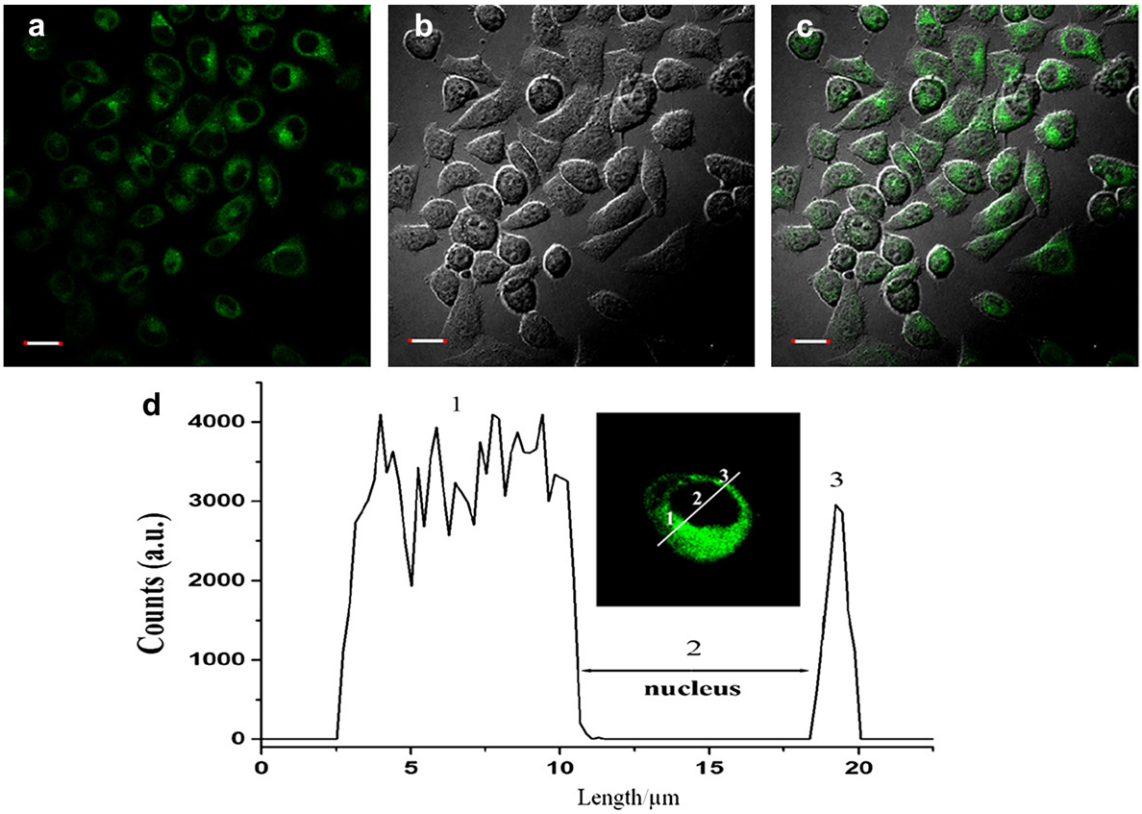

Fig. 2. Confocal fluorescence (a), bright-field (b) and overlay (c) images of KB cell stained with 2.5 μM **3** for 15 min at 37 °C. Fluorescence intensity profile across the line shown in cell image is shown in (d). All excitation wavelengths are 405 nm. Scale bar = 20 μm.

process of cercariae was observed for 4 h (Fig. 3). **3** was rapidly taken up by cercariae through the tegument at 10 min, but its fluorescence intensity was very low (Fig. 3a). Then, fluorescence intensity in the cercarial body continually increased in the period from 30 min to 2 h (Fig. 3b–d), indicating that the movement of compound **3** occurred as a result of the parasite's somatic circulation. These facts also indicated that **3** could penetrate into the cercarial body and act on inner organs.

To further understand the drug's action in cercariae, we also carried out a control experiment using fluorophore **6**. We selected images respectively stained by **3** and **6** after 4 h (Fig. 4). The fluorescence signal of **6** was localized around the ventral sucker or pre-acetabular gland and post-acetabular gland, but the fluorescence signal was remarkably weak in other parts (Fig. 4b). In contrast, **3**-labelled cercariae showed strong fluorescence signal which was localized not only in the pre-acetabular gland and post-acetabular gland, but also in the head organ and tail (Fig. 4a). A further exploration of the staining of cercariae by **3** was carried out by three-dimensional (3D) visualization. The fluorescence intensity of **3**-stained cercariae was stronger than that of fluorophore-**6**-stained cercariae. It is deduced that **3** easily enters into the cercarial body and distributes uniformly. This result is in agreement with previous studies by Merschjohann et al., [7] to a certain extent, which finds that niclosamide can penetrate into the body of rats elsewhere beyond the circulatory system. We could deduce that **3** was effectively absorbed by cercariae through its tegument, which led to cercaria's rapid death.

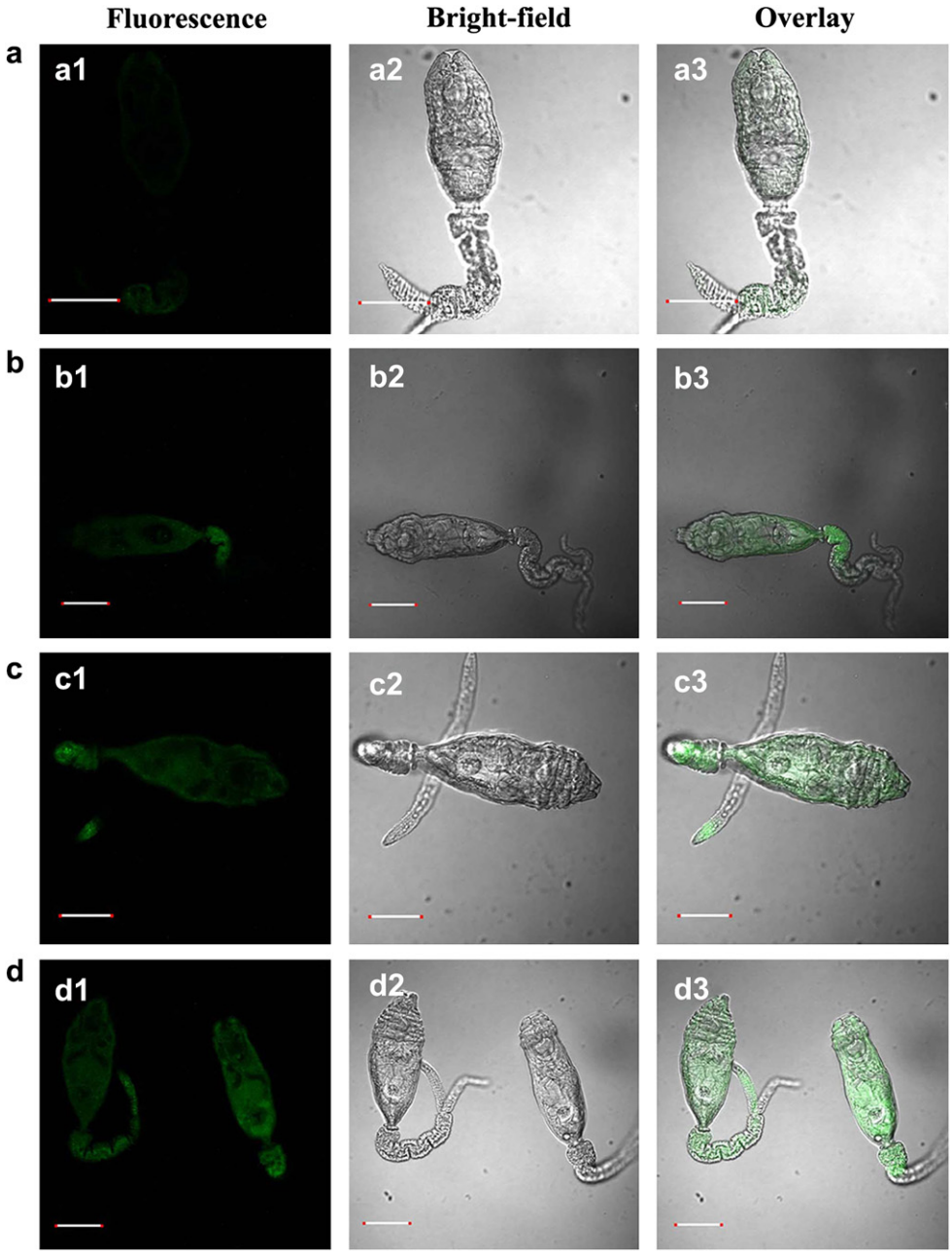

Fig. 3. Confocal fluorescence, bright-field and overlay images of cercariae incubated with compound **3** (5 μM) in PBS buffer at room temperature for 10 min (a), 30 min (b), 1 h (c) and 2 h (d). All excitation wavelengths are 405 nm. Scale bars = 20 μm.

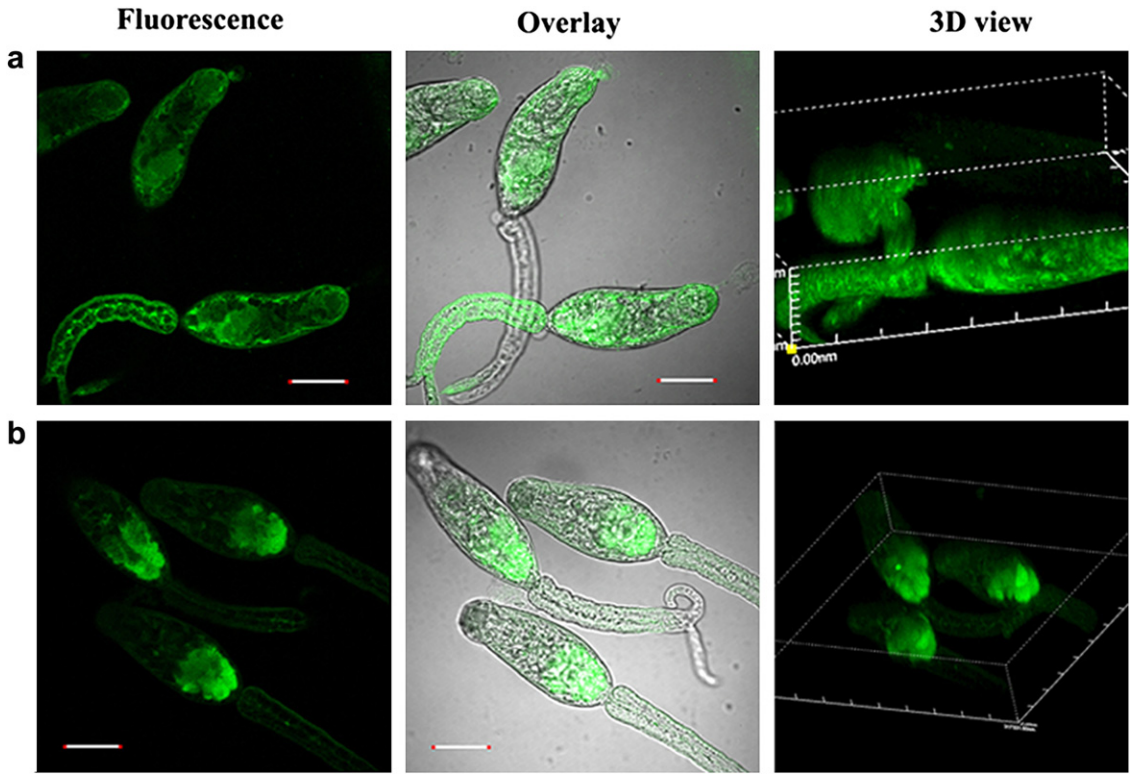

Fig. 4. Confocal fluorescence, overlay and three-dimensional (3D) fluorescence images of cercariae stained by **3** (a, top) and **6** (b, bottom) for 4 h. All excitation wavelengths are 405 nm. Scale bars = 20 μm.

4. Conclusions

In summary, the novel derivative of niclosamide **2b** possesses properties of self-diffusion, water-surface floating and excellent bioactivity against *S. japonicum* cercariae at low concentration. Fluorescence imaging experiments proved that **3** can be rapidly absorbed by the parasitic body through the tegument. This study provides a foundation for investigating the preliminary mode of niclosamide action in *S. japonicum* cercariae. It is the first investigation of the distribution of niclosamide derivatives in *S. japonicum* cercariae by fluorescence imaging. Possible bioactivities of **2a**/**2b** against *O. hupensis* are also currently being investigated.

Acknowledgements

The authors are grateful for the financial support from The National Natural Science Foundation of China (NSFC, 50727803 and 50968002), National Key Technologies R&D Program (2009BAI78B01) and Shanghai Leading Academic Discipline Project (B108).

Appendix. Supplementary data

Supplementary data associated with this article can be found in the online version, at doi:10.1016/j.dyepig.2010.08.002.

References

[1] Hotez PJ, Molyneux DH, Fenwick A, Kumaresan J, Sachs SE, Sachs JD, et al. Control of neglected tropical diseases current concepts. New England Journal of Medicine 2007;357:1018–27.
[2] Chitsulo L, Engels D, Montresor A, Savioli L. The global status of Schistosomiasis and its control. Acta Tropica 2000;77:41–51.
[3] Hugo VB. Chemotherapy of parasitic infections. Nature 1978;273:626–30.
[4] King CH, Dickman K, Tisch DJ. Reassessment of the cost of chronic helmintic infection: a meta-analysis of disability-related outcomes in endemic schistosomiasis. Lancet 2005;365:1561–9.
[5] Savioli L, Engels D, Roungou JB, Fenwick A, Endo H. Schistosomiasis control. Lancet 2004;363:658.
[6] Cherfas J. New weapon in the war against Schistosomiasis. Science 1989;246 (4935):1242–3.
[7] Merschjohann K, Steverding D. In vitro trypanocidal activity of the anthelminthic drug niclosamide. Experimental Parasitology 2008;118:637–40.
[8] Lowe D, Xi JY, Meng XH, Wu ZS, Qiu DC, Spear R. Transport of Schistosoma japonicum cercariae and the feasibility of niclosamide for cercariae control. Parasitology International 2005;54:83–9.
[9] Devarakonda B, Hill RA, Liebenberg W, Brits M, Villiers MM. Comparison of the aqueous solubilization of practically insoluble niclosamide by polyamidoamine (PAMAM) dendrimers and cyclodextrins. International Journal of Pharmaceutics 2005;304:193–209.
[10] Akelah A, Reha A. Polymeric molluscicides containing niclosamide moieties. Materials Science and Engineering C 1996;4:1–5.
[11] Gnoula C, Guissou I, Dubois J, Duez P. 5(6)-Carboxyfluorescein diacetate as an indicator of *Caenorhabditis elegans* viability for the development of an in vitro anthelmintic drug assay. Talanta 2007;71:1886–92.
[12] Keeney DB, Lagrue C, Bryan-Walker K, Khan N, Leung TLF, Poulin R. The use of fluorescent fatty acid analogs as labels in trematode experimental infections. Experimental Parasitology 2008;120:15–20.
[13] Weissleder R, Pittetl MJ. Imaging in the era of molecular oncology. Nature 2008;452(3):580–9.
[14] Bringmann G, Gampe CM, Reichert Y, Bruhn T, Faber JH, Mikyna M, et al. Synthesis and pharmacological evaluation of fluorescent and photoactivatable analogues of antiplasmodial naphthylisoquinolines. Journal of Medicinal Chemistry 2007;50:6104–15.
[15] Imming P, Sinning C, Meyer A. Drugs, their targets and the nature and number of drug targets. Nature Reviews Drug Discovery 2006;5:821–34.
[16] Stoll I, Eberhard J, Brodbeck R, Eisfeld W, Mattay J. A new fluorescent calix crown ether: synthesis and complex formation with alkali metal ions. Chemistry – A European Journal 2008;14:1155–63.
[17] Kumar S, Ramachandran U. The synthesis and applications of asymmetric phase-transfer catalysts derived from isomannide and isosorbide. Tetrahedron 2005;61:4141–8.
[18] Mandl CP, Knig B. Luminescent crown ether amino acids: selective binding to *N*-terminal lysine in peptides. Journal of Organic Chemistry 2005;70:670–4.
[19] Wu JC, Yi T, Shu TM, Yu MX, Zhou ZG, Xu M, et al. Ultrasound switch and thermal self-repair of morphology and surface wettability in a cholesterol-based self-assembly system. Angewandte Chemie International Edition 2008;47:1063–7.

[20] DeSilva AP, Nimal Gunaratne HQ, Habib-Jiwan JL, McCoy CP, Rice TE, Soumilion JP. New fluorescent model compounds for the study of photoinduced electron transfer: the influence of a molecular electric field in the excited state. Angewandte Chemie International Edition 1995;34:1728–31.
[21] Bojinov VB, Panova IP. Novel 4-(2,2,6,6-tetramethylpiperidin-4-ylamino)-1,8-naphthalimide based yellow-green emitting fluorescence sensors for transition metal ions and protons. Dyes and Pigment 2009;80:61–6.
[22] Hassheider T, Benning S, Kitzerow HS, Achard MF, Bock H. Color-tuned electroluminescence from columnar liquid crystalline alkyl arenecarboxylates. Angewandte Chemie International Edition 2001;40:2060–3.
[23] Li HJ, Liang YS, Dai JR, Xu YL, Tang JX, Ru WW, et al. Study on killing effect of suspension concentrate of niclosamide against cercariae of *Schistosoma japonicum*. Chinese Journal of Schistosomiasis Control 2005;17 (6):424–6.